

J. Harle[†], Adrian New[†], W. Norton^{*}, L. Shaffrey^{*}, D. Stevens^{**}, I. Stevens^{**}, J. Slingo^{*}

[†] National Oceanography Centre, Southampton. ^{*} Centre for Global Atmospheric Modelling, University of Reading. ^{**} School of Mathematics, University of East Anglia

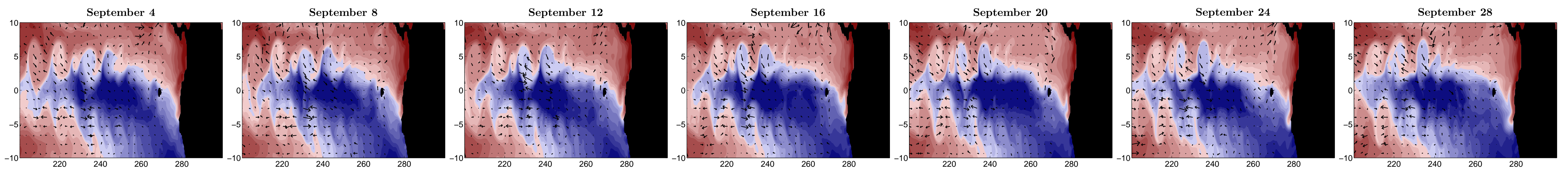


Figure 1: Time-series of daily mean Sea Surface Temperature with TIW induced wind stress vectors overlaid (temperature range -20-30°C).

Abstract

The High resolution Global Environmental Model (HiGEM) is a fully coupled global climate model of hitherto unprecedented resolution. Processes which participate in air-sea interaction are examined in the model. In particular, the model is of sufficient resolution to realistically simulate Tropical Instability Waves (TIWs) in the eastern tropical Pacific. The strong sea surface temperature gradients drive perturbations in the overlying wind field with a lag of a few days, and the whole system propagates westwards along the equator. The mechanisms involved in such ocean-atmosphere coupling and their implications are examined.

Introduction

Tropical Instability Waves (TIW) are cusp-like features that appear along the northern and southern boundaries of the eastern tropical Pacific cold tongue. They propagate westward with a phase speed of $\sim 0.5 \text{ m s}^{-1}$ and have typical wavelengths of 1000 to 2000 km (e.g. Contreras, 2002). These properties vary seasonally and interannually depending on the prominence of the cold tongue. The properties of TIWs in our climate model fall within the bounds of observations (1400 km and 0.6 m s^{-1} during the boreal autumn, Figure 1).

Observational studies have found that Sea Surface Temperature (SST) perturbations associated with TIWs cause fluctuations in surface winds (e.g. Chelton et al., 2001, see Figure 1). The effect of the SSTs on the atmospheric boundary layer (ABL) is to increase the wind over warm water and decrease it over cool. The difference in wind speeds either side of SST fronts, such as those found in the tropical Pacific, lead to an anomalous divergence and curl in surface wind stress (Figure 2).

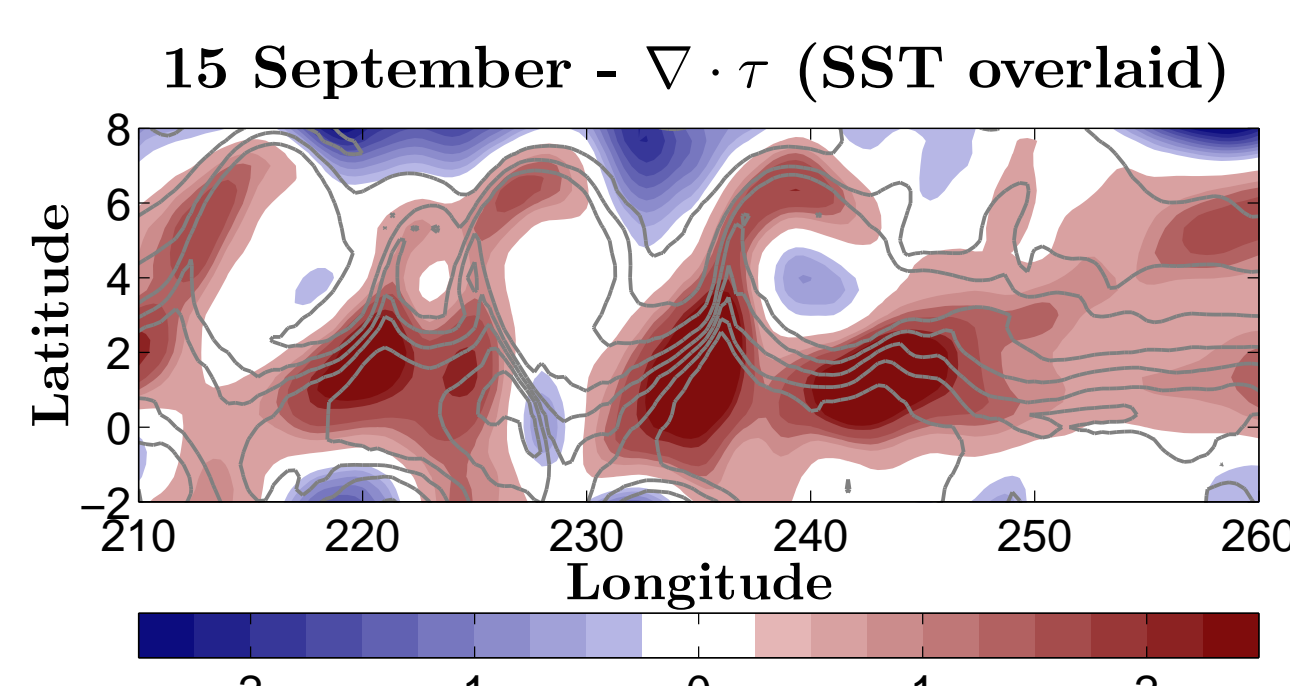


Figure 2: Daily mean wind stress divergence (Nm^{-2} per 10^4 km). Associated SST contours are overlaid ($^{\circ}\text{C}$).

Model

HiGEM is a high resolution coupled climate model that has been developed from the Hadley Centres HadGEM model. Along with modified physics and numerics, the resolution of the ocean has been increased from 1° to $\frac{1}{3}^{\circ}$ and the atmosphere from $1\frac{1}{8}^{\circ} \times 1\frac{1}{4}^{\circ}$ to $1\frac{1}{4}^{\circ} \times \frac{2}{6}^{\circ}$. The ocean has 40 depth levels and bathymetry derived from the GEBCO data set, which was subsequently modified in flow sensitive regions. The atmosphere model has 38 levels, 8 of these are in the atmospheric boundary layer. Atmosphere and ocean are coupled once a day. For further information on HiGEM please see Ian Stevens' poster: *Results from a high resolution coupled climate model* (No. 118).

Validation

Following the observational study of Chelton et al. (2001) we assess the performance of our model with respect to the local coupling of TIWs and the overlying wind field. Chelton et al. find the wind stress derivatives to be linearly related to the SST gradient:

$$\nabla T \cdot \hat{\tau} \propto \nabla \cdot \tau \quad \nabla T \times \hat{\tau} \propto \nabla \times \tau$$

where the downwind temperature gradient and crosswind temperature gradient can be derived by:

$$\nabla T \cdot \hat{\tau} = |\nabla T| \cos \theta \quad \nabla T \times \hat{\tau} \cdot \hat{k} = |\nabla T| \sin \theta$$

θ being the counterclockwise angle between the SST gradient vector and the wind stress vector. As we are only concerned with the TIW-perturbed wind stress divergence and wind stress curl, a zonal high-pass filter is employed to isolate the TIW signatures from the large-scale variability. The resulting perturbation fields are denoted by a prime.

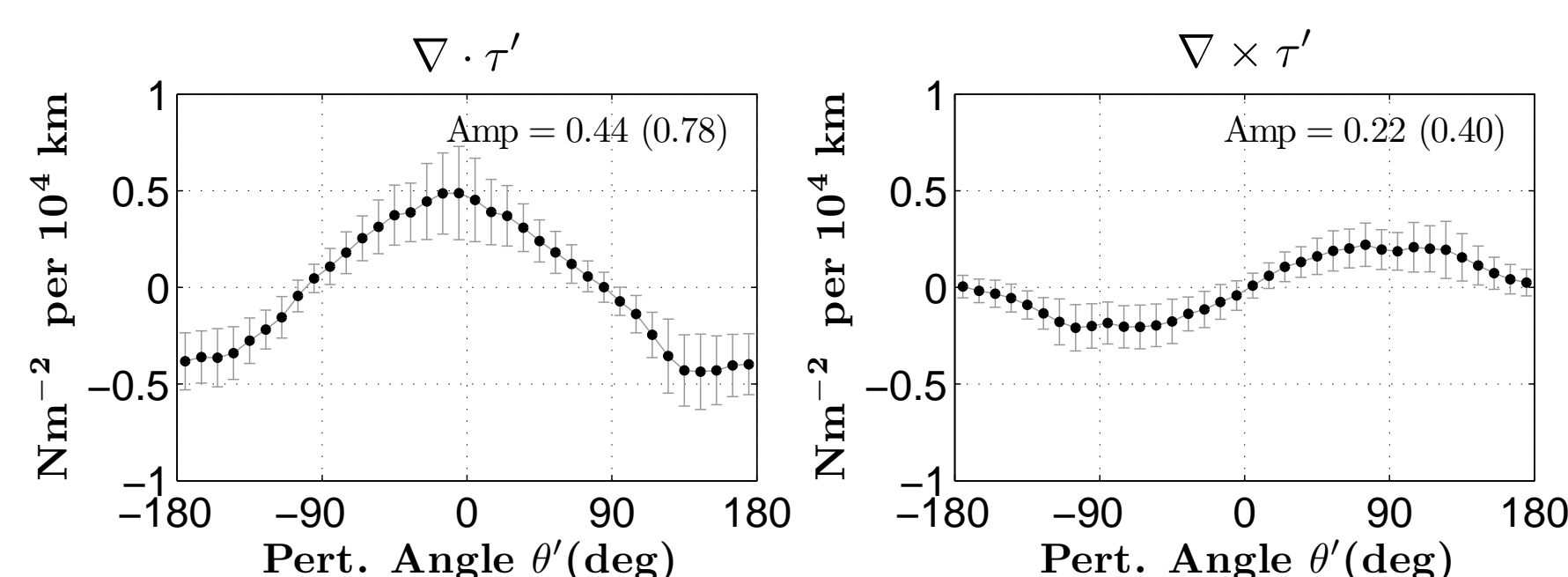


Figure 3: Angular dependencies of perturbations in (left) wind stress divergence and (right) wind stress curl. Chelton et al.'s values given in parentheses.

The perturbation angle is given by:

$$\theta' = \tan^{-1} \left[\frac{(\nabla T \times \hat{\tau})' \cdot \hat{k}}{(\nabla T \cdot \hat{\tau})'} \right]$$

The response of the wind field perturbations to the perturbations in the SST gradient are shown in Figure 3. The wind stress divergence perturbation exhibits a cosine response (i.e. as $(\nabla T \cdot \hat{\tau})' \rightarrow 0$, $|\nabla \cdot \tau'|$ is maximum) and the curl a sine response (i.e. as $(\nabla T \cdot \hat{\tau})' \rightarrow 0$, $|\nabla \times \tau'|$ is maximum).

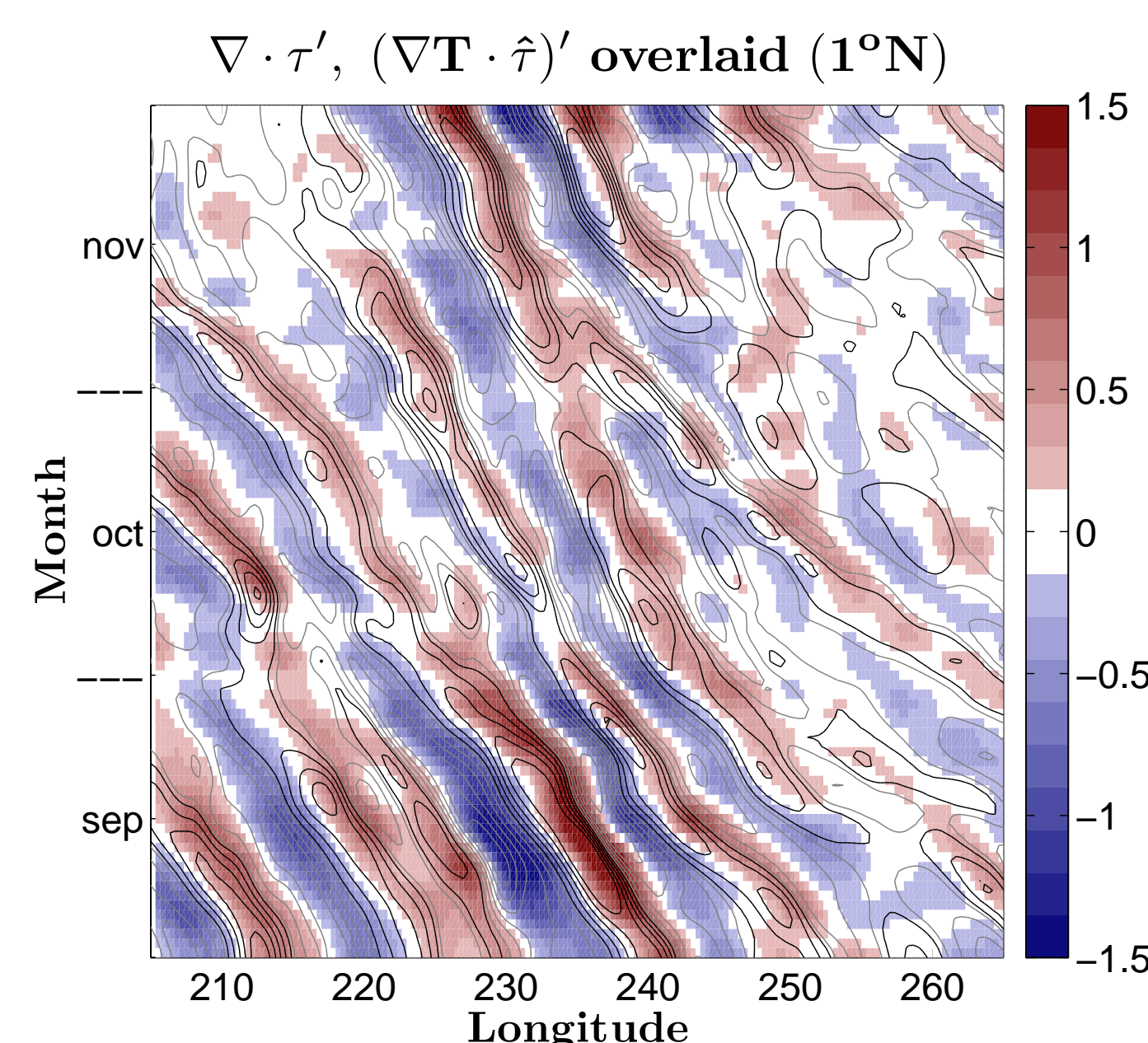


Figure 4: Longitude-Time plot of $\nabla \cdot \tau'$ along 1°N . Overlaid are contours of $(\nabla T \cdot \hat{\tau})'$ (black contours - positive, grey - negative).

The westward propagation of the downwind (crosswind) SST gradient perturbation and wind stress divergence (curl) perturbation is clearly seen in Figure 4 (crosswind and curl fields not shown). However, it appears that either the signals are not co-located in space or time or both. It is unclear whether this feature is a result of the once-a-day coupling or that the two signals are just not co-located in space as in the observations. Simulations using higher frequency coupling are currently under way to resolve this question.

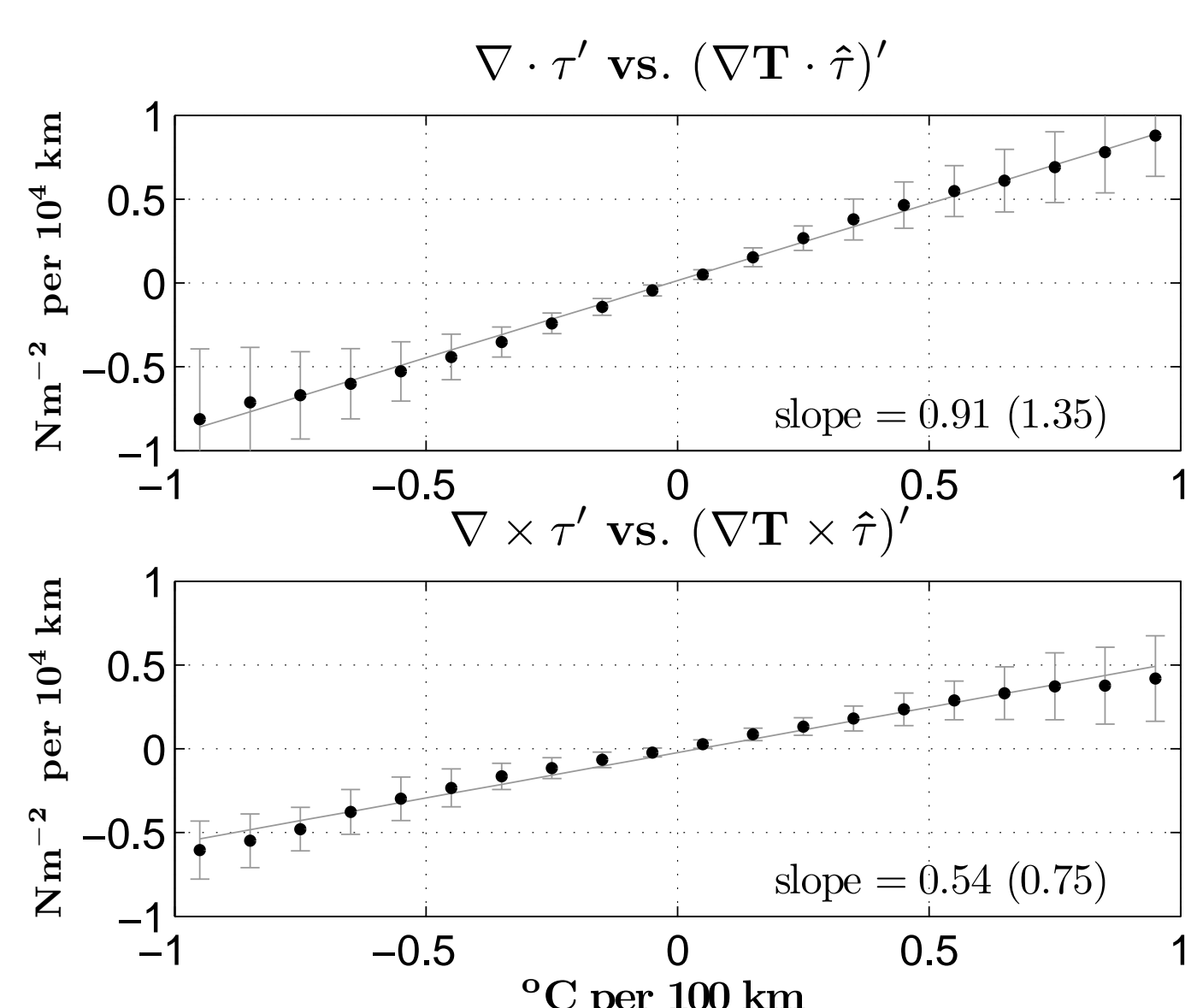


Figure 5: Relationship between the perturbation in the downwind (crosswind) SST gradient and the perturbation in wind stress divergence (curl). Chelton et al.'s values given in parentheses

The strength of the coupling between SST gradient and surface wind field is implied by the slope of the least squares straight line fit to the binned averages of the two fields (Figure 5). It appears that the model is performing well in this respect simulating a TIW induced perturbation in the wind field.

Response

Two mechanisms by which the wind field responds to the TIW induced SST anomalies are proposed by Hayes et al. (1989) and Lindzen and Nigam (1987). The first is through vertical mixing of momentum from winds aloft as the ABL is destabilised over the warmer SSTs. The second is that SST variations induce sea level pressure (SLP) anomalies through hydrostatic balance, resulting in converging (diverging) winds over warm (cold) anomalies.

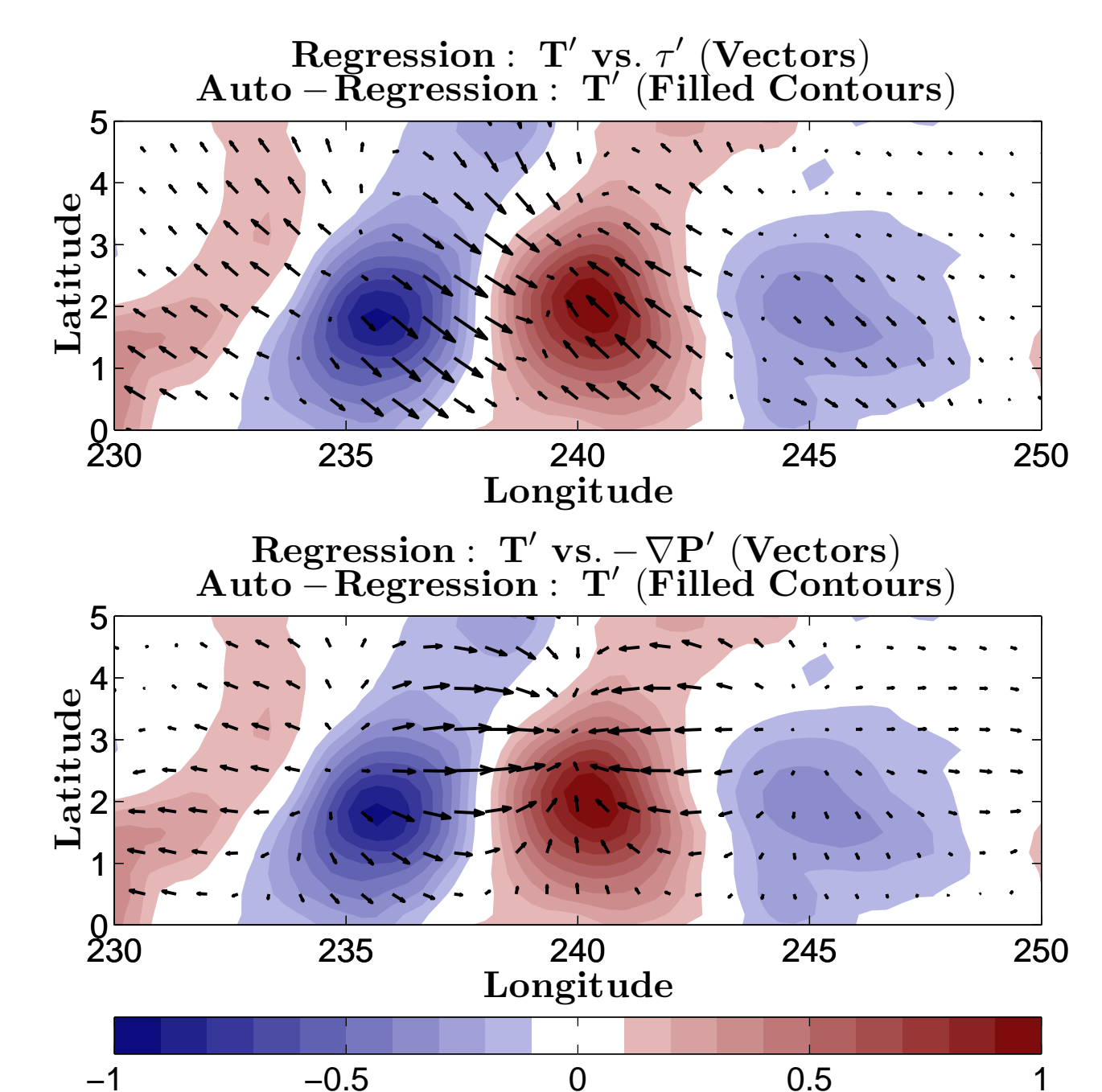


Figure 6: Linear regression of (top) wind stress perturbation and (bottom) pressure gradient term against the SST perturbation (normalised vector arrows).

We can examine the relationship between ocean and atmosphere by regressing certain atmospheric fields onto the underlying SST field. It is anticipated that using this method we can ascertain which of the two proposed mechanisms is dominant in HiGEM. Figure 6 shows two examples. The first is of wind stress perturbation regressed against a reference SST perturbation time series at 2°N , 240°E . The second is of the pressure gradient term in the momentum balance, also regressed against the same SST time-series. This shows SLP anomalies, indicated by points of convergence (divergence), do not occur directly above the SST anomalies, as suggested by Lindzen and Nigam (1987), but to the north-west of them (downwind). Further model runs are required to fully diagnose all the terms in the momentum balance and to shed more light on the mechanisms involved in TIW modification of the ABL.

Summary

- The response of the wind field to TIW induced SST anomalies is not as strong as in the observations, however the strength of the coupling is comparable. Although the model is still limited by resolution we have shown that it provides a sufficient tool to study air-sea interactions in the eastern tropical Pacific. Something that previous coarser resolution climate models have been unable to do.
- High frequency coupling experiments are underway to further quantify the observed lags between the SST gradient and the wind field derivatives. Extra diagnostics have also been included to determine the governing mechanism of the wind field response.
- We will carry out a series of sensitivity experiments to determine whether these local air-sea interactions have a significant impact on the mean state of the climate system.

References

- Chelton, D. B. et al., *J. Clim.*, 14(7):1479-1498, 2001.
Contreras, R. F., *J. Phys. Oceanogr.*, 32(9):2715-2722, 2002.
Hayes, S. P. et al., *J. Clim.*, 2(12):1500-1506, 1989.
Lindzen, R. S. and S. Nigam, *J. Atmos. Sci.*, 44(17):2418-2436, 1987.

This work was supported through a consortium project funded by the Natural Environmental Research Council.

Corresponding author address: James Harle, National Oceanography Centre, Southampton, SO14 3ZH, U.K.
Email: jdha@noc.soton.ac.uk